Available online at http://www.journalijdr.com

International Journal of DEVELOPMENT RESEARCH

ISSN: 2230-9926

International Journal of Development Research
Vol. 06, Issue, 12, pp.10575-10581, December, 2016

Full Length Research Article

CHEMICAL REACTION EFFECTS ON MICROPOLAR NANOFLUID FLOW OVER A MHD RADIATIVE STRETCHING SURFACE WITH THERMAL CONDUCTIVITY

*[1]Srinivas Maripala and [2]Kishan Naikoti

[1]Department of Mathematics, Sreenidhi Institute of Science and Technology, Ghatkesar, Hyd-501301
[2]Department of Mathematics, Osmania University, Hyd-07

ARTICLE INFO

Article History:

Received 25th September, 2016
Received in revised form
22nd October, 2016
Accepted 19th November, 2016
Published online 30th December, 2016

Key Words:

MHD,
Microrotation Parameter,
Radiation Parameter,
Eckert Number,
Thermal Conductivity Parameter,
Brownian Motion Parameter,
Thermophoresis Parameter.

ABSTRACT

In this paper, an analysis is presented the effects of chemical reaction parameter variable thermal conductivity and radiation on the flow and heat transfer of an electrically conducting micropolar nanofluid over a continuously stretching surface with varying temperature in the presence of a magnetic field. The surface temperature is assumed to vary as a power-law temperature. The governing conservation equations of mass, momentum, angular momentum and energy are converted into a system of non-linear ordinary differential equations by means of similarity transformation. The resulting system of coupled non-linear ordinary differential equations is solved by implicit finite difference method. The results are analyzed for the effect of different physical parameters such as magnetic parameter, microrotation parameter, Prandtl number, radiation parameter, Eckert number, thermal conductivity parameter, Brownian motion parameter, Thermophoresis parameter, Lewies number, surface temperature parameter on the velocity, angular velocity, temperature and concentration fields are presented through graphs. Physical quantities such as skin friction coefficient, local heat, local mass fluxes are also computed and are shown in table.

INTRODUCTION

The enhancement of thermal conductivity in nanofluids has attracted the interest of many researchers. A detailed survey of convective heat transfer in nanofluids by Buongiorno [1] predicted that the nanoparticles' absolute velocity is roughly a sum of the base fluid velocity and the slip velocity. He focused on inertia, Brownian diffusion, thermopharesis, diffusiopharesis, Magnus effect, fluid drainage, and the gravity setting as the effective quantities and concluded that for the laminar type flow, only the Brownian diffusion and the thermopharesis have noticeable effects. Using the Boungiorno (Buongiorno, 2006) model, Kuznetseov and Nield (2010) studied the influence of nanoparticles on a natural convection boundary layer flow passing a vertical plate. They considered the temperature and nanoparticle fraction both to be constant along the wall and concluded that the reduced Nusselt number is a decreasing function of the nanofluid numbers Nr, Nb and Nt. Nield and Kuznetseov (2009) have examined the onset of convection in a horizontal layer of a porous medium layer saturated by a nanofluid through the use of linear instability theory. Moreover, the onset of convection in a horizontal layer uniformly heated from the bottom, known as the Benard problem, was studied by Tzou (2008). The mixed convection boundary layer flow passing a vertical flat plate embedded in a porous medium filled with a nanofluid (the basic fluid was considered to be water) was studied by Ahmad and Pop (2010). Furthermore, Eastman et al. (2001) used pure copper nanoparticles of size less than 10nm and achieved an increase of 40 in thermal conductivity for only 0.3 volume fraction of the solid dispersed in ethyleneglycal. The theory of thermomicropolar fluids was developed by Eringen (1972) by extending his theory of micropolar fluid. The flow characteristics of the boundary layer of micropolar fluid over a semi-infinite plate in different situations have been studied by many authors. Recently, Srinivas Maripala and Kishan Naikoti (Srinivas Maripala and Kishan Naikoti, 2016) studied the thermal radiation effects on MHD flow of a micropolar fluid over a stretching surface with variable thermal conductivity .

Basic equations

Consider a steady two-dimensional flow of an incompressible, electrically conducting micropolar nanofluid, subject to a transverse magnetic field over a semi-infinite stretching plate with variable temperature in the presence of radiation.

***Corresponding author: Srinivas Maripala,**
Department of mathematics, Sreenidhi Institute of Science and Technology, Ghatkesar, Hyd-501301.

The x-axis is directed along the continuous stretching plate and points in the direction of motion. The y-axis is perpendicular to x-axis and to the direction of the slot (the z-axis) whence the continuous stretching plate issues. It is assumed that the induced magnetic field and the Jole heating are neglected. The fluid properties are assumed to be constant, except for the fluid thermal conductivity which is taken as a linear function of temperature. Then under the usual boundary layer approximations, the governing equations for the problem can be written as follows (Raptis, 1998):

$$\frac{\partial u}{\partial x}+\frac{\partial v}{\partial y}=0 \tag{1}$$

$$u\frac{\partial u}{\partial x}+v\frac{\partial u}{\partial y}=v\frac{\partial^2 u}{\partial y^2}+K_1\frac{\partial \sigma}{\partial y}-\frac{\sigma B_0^2}{\rho}u \tag{2}$$

$$G_1\frac{\partial^2 \sigma}{\partial y^2}-2\sigma-\frac{\partial u}{\partial y}=0 \tag{3}$$

$$\rho c_p\left(u\frac{\partial T}{\partial x}+v\frac{\partial T}{\partial y}\right)=\frac{\partial}{\partial y}\left(k\frac{\partial T}{\partial y}\right)+\mu\left(\frac{\partial u}{\partial y}\right)^2-\frac{\partial q_r}{\partial y}+\tau\left[D_B\frac{\partial C}{\partial y}\frac{\partial T}{\partial y}+\frac{D_T}{T_\infty}\left(\frac{\partial T}{\partial y}\right)^2\right] \tag{4}$$

$$\frac{\partial C}{\partial t}+u\frac{\partial C}{\partial x}+v\frac{\partial C}{\partial y}=D_B\frac{\partial^2 C}{\partial y^2}+\frac{D_T}{T_\infty}\frac{\partial^2 T}{\partial y^2}--k_c(C-C_\infty) \tag{5}$$

where $v=(\mu+S)/\rho$ is the apparent kinematic viscosity, μ is the coefficient of dynamic viscosity, S is a constant characteristic of the fluid, σ is the microrotation component, $K_1=S/\rho(>0)$ is the coupling constant, $G_1(>0)$ is the microrotation constant, ρ is the fluid density, u and v are the components of velocity along x and y direction, respectively. T is the temperature of the fluid in the boundary layer, T_∞ is the temperature of the fluid far away from the plate, T_w is the temperature of the plate, k is the thermal conductivity, c_p is the specific heat at constant pressure, σ_0 is the electric conductivity, B_0 is an external magnetic field and q_r is the radiative heat flux. *T* is the temperature, C is the concentration of the fluid, C_p is the specific heat, q_r is the radiative heat flux, $K_c$is chemical reaction parameter, T_w and C_w - the temperature and concentration of the sheet, T_∞ and C_∞- the ambient temperature and concentration, D_B - the Brownian diffusion coefficient, D_T the thermophoresis coefficient, B_0 - the magnetic induction, $(\rho C)_p$ - the heat capacitance of the nanoparticles, $(\rho C)_f$- the heat capacitance of the base fluid, and $\tau=(\rho C)_p/(\rho C)_f$ is the ratio between the effective heat capacity of the nanoparticles material and heat capacity of the fluid.

The boundary conditions of the problem are given by

$$y=0\ \ u=\propto x\ \ v=0\ \ T=T_w(x)\ \ \sigma=0$$
$$y\to\infty,\ u\to 0\ \ T\to T_\infty,\ \sigma\to 0 \tag{6}$$

The wall temperature is assumed to vary along the plate according to the following power-law

$$T_w-T_\infty=\beta x^\gamma \tag{7}$$

where β and γ (the surface temperature parameter) are constants. The fluid thermal conductivity is assumed to vary as a linear function of the temperature in the form (Slattery, 1972)

$$k=k_\infty\left[1+b[(T-T_\infty)]\right] \tag{8}$$

where b is a constant depending on the nature of the fluid and k_∞ is the ambient thermal conductivity. In general, b>0 for air and liquids such as water, while b<0 for fluids such as lubrication oils. Using Rosselant approximation (Sparrow and Cess, 1978) we have

$$q_r=(-4\sigma^*/3k^*)\frac{\partial T^4}{\partial y} \tag{9}$$

where σ^* is the Stefan Boltzmann constant and k^* is the mean absorption coefficient. In this study, we consider the case where the temperature differences within the flow are sufficiently small. Expanding T^4in a Taylor series about T_∞ and neglecting higher order terms (Raptis, 1998), we have

$$T^4\cong 4T_\infty^3\,T-3T_\infty^4 \tag{10}$$

Using Eq.(8), Eq.(4) becomes

$$\rho c_p\left(u\frac{\partial T}{\partial x}+v\frac{\partial T}{\partial y}\right)=\frac{\partial}{\partial y}\left(k\frac{\partial T}{\partial y}\right)+\mu\left(\frac{\partial u}{\partial y}\right)^2+\frac{16\sigma^* T_\infty^3}{3k^*}\frac{\partial^2 T}{\partial y^2}+\tau\left[D_B\frac{\partial C}{\partial y}\frac{\partial T}{\partial y}+\frac{D_T}{T_\infty}\left(\frac{\partial T}{\partial y}\right)^2\right] \tag{11}$$

by using the following similarity transformations

$$\eta = (a/v)^{\frac{1}{2}}\, y \,,\quad \psi = (av)^{\frac{1}{2}}\, x\, f(\eta)$$

$$u = \frac{\partial\psi}{\partial y},\quad v = -\frac{\partial\psi}{\partial x},\quad \sigma = (a^3/v)^{1/2} x g(\eta),\quad \theta(\eta) = \frac{T-T_\infty}{T_w-T_\infty},\quad k = k_\infty(1+S\theta) \tag{12}$$

Substituting fromEq.(12) into Eqs.(1)-(3) and (10), we have

$$f''' + ff'' - f'^2 + G_1 g' - Mf' = 0 \tag{13}$$

$$G\, g'' - (2g + f'') = 0 \tag{14}$$

$$[4 + 3F(1+S\theta)]\theta'' + 3FPr[f\theta' - \gamma f'\theta + Ec(f'')^2 + 3FS(\theta'')^2 + \Pr[Nb\,\theta'\varphi' + Nt\,\theta'^2] = 0 \tag{15}$$

$$\varphi'' - Le\, f\varphi' + \frac{Nt}{Nb}\theta'' - K\varphi = 0 \tag{16}$$

Where

$G_1 = K_1/v$ (coupling constant parameter), $M = (\sigma_0 B_0^2)/\rho a$ (magnetic parameter), $G = G_1\, \alpha/v$ (microrotation parameter), $P_r = (\mu c_p)/k_\infty$ (Prandtl number), $F = (k_\infty k^*)/(4\sigma^* T_\infty^3)$ (Radiation parameter), $Ec = \frac{\alpha^2 x^2}{c_p(T_w - T_\infty)}$ (Eckert number), $S = b(T_w - T_\infty)$ (thermal conductivity parameter), $Nb = \tau D_B(C_w - C_\infty)/v$ (Brownian motion parameter), $Nt = \tau D_T(T_w - T_\infty)/vT_\infty$ (Thermophoresis parameter), $Le = v/D_B$ (Lewies number), γ = Surface temperature parameter

For air $0 \le S \le 6$, for water $0 \le S \le 0.12$ and for lubrication oils $-0.1 \le S \le 0$ [11]

The transformed boundary conditions are given by

$$f(0) = 0,\ f'(0) = 1,\ \theta(0) = 1,\ g(0) = 0,$$

$$f'(\infty) = 0,\ \theta(\infty) = 0,\ g(\infty) = 0 \tag{17}$$

From the velocity field we can study the wall shear stress, τ_w as given by [12]:

$$\tau_w = -\left|\ (\mu + S)\frac{du}{dy} + S\sigma\ \right|\ at\ y = 0 \tag{18}$$

The skin frication coefficient c_f is given by

$$c_f = \left(\frac{2\tau}{\rho u^2}\right)_{y=0} = -2R_{ex}^{-1/2} f''(0) \tag{19}$$

where $R_{ex} = ax/v$ is the local Reynolds number. Eq. (20) shows the skin frication coefficient does not contain the microrotation term in an explicitly way.

The rate of heat transfer is given by

$$q_w = -k\left(\frac{\partial T}{\partial y}\right) at\ \ y = 0 \tag{20}$$

The local heat transfer coefficient is given by

$$h(x) = q_w\ /T_w - T_\infty \tag{21}$$

The local Nusselet number is known as

$$N_{ux} = \frac{hx}{k} = -R_{ex}^{\frac{1}{2}}\theta'(0) \tag{22}$$

The couple stress is given by

$$m_w = G_1\ \left(\frac{\partial\sigma}{\partial y}\right)_{y=0} = R_{ex}\ \left(\frac{G_1 a}{x}\right) g'(0) \tag{23}$$

M	F	γ	S	$-f''(0)$	$g'(0)$	$-\theta'(0)$	$-\varphi'(0)$
0.0	1.0	1.0	0.1	1.12845	0.261526	0.369843	0.35294
3.0	3.0	1.5	0.2	1.52926	0.294128	0.291427	029129
5.0	5.0	2.0	0.5	2.30121	0.351692	0.243161	0.24321

RESULTS AND DISCUSSION

In order to solve the non-linear coupled equations (13) – (16) along with boundary conditions (17) an implicit finite difference scheme of Cranck-Nicklson type has been employed. The computations have been carried out for various flow parameters such as magnetic parameter *M*, microrotation parameter *G*, Prandtl number *Pr*, radiation parameter *F*, Eckert number *Ec*, thermal conductivity parameter *S*, Brownian motion parameter *Nb*, Thermophoresis parameter *Nt*, Lewies number *Le*, surface temperature parameter γ on the velocity, angular velocity, temperature and concentration fields are presented through graphs. Physical quantities such as skinfrication coefficient $f''(0)$, the couple stress coefficient $-g'(0)$, local nusselet number $\theta'(0)$, and Sherwood parameter $\varphi'(0)$) are also computed and are shown in table.

It is evident that with the increase of magnetic parameter *M*, radiation parameter *F*, surface temperature γ and thermal radiative parameter *S*, increases skin frication coefficient $f''(0)$, and couple stress coefficient $-g'(0)$, decreases the local nusselet number $\theta'(0)$ and Sherwood parameter $\varphi'(0)$. It is observed from Figure 1(a)-1(d), that an increase in magnetic parameter *M* leads to a decrease in velocity profiles f' and angular velocity *g*. The velocity boundary layer thickness becomes thinner as *M* increases. This is due to the fact that applications of a magnetic field to an electrically conductivity fluid produce a drag-like force called Lorentz force. This force causes reduction in the fluid velocity.

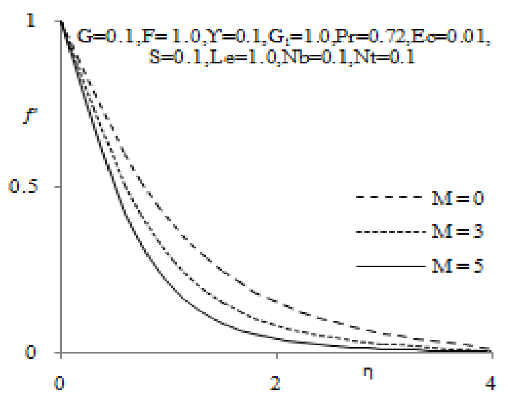

1(a). Velocity distribution for various values of M

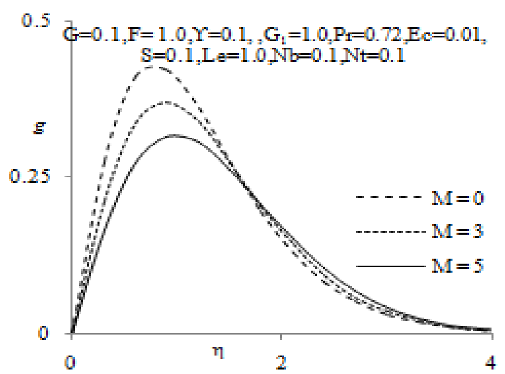

1(b). Angular velocity distribution for various values of M

The thermal boundary layer thickness increases with increasing the magnetic parameter *M* has shown in Figure 1(c). The reason for this behavior is that the Lorentz force increases the temperature. The concentration profiles are increased with the increase of magnetic field parameter *M*, is observed from Figure 1(d). The effect of Brownian motion parameter *Nb* on velocity, temperature and concentration profiles are shown in figures 2(a) - 2(c). The velocity profiles are decreased with the increase of Brownian motion parameter *Nb.* As expected, the boundary layer profiles for the temperature are of the same form as in the case of regular heat transfer fluids.

Temperature in the boundary layer increases and the nanoparticle volume fraction decreases with the increase in Brownian motion parameter. Brownian motion serves to warm the boundary layer and simultaneously exacerbates particle deposition away from the fluid regime or onto the surface, thereby accounting for the reduced concentration magnitudes. For small particles, Brownian motion is strong and the parameter *Nb* will have high values, the converse is the case for large particles and clearly Brownian motion does exert a significant enhancing influence on both temperature and concentration profiles.

Figure 2(b), illustrates that the temperature profiles are increased as Brownian motion parameter *Nb* increases. Concentration profiles are decreased, when Brownian motion parameter *Nb* increases is observed from the Figure 2(c). Figures 3(a)-3(c) present typical profile for temperature and concentration for various values of thermophoretic parameter *Nt*. It is observed that an increase in the thermophoretic parameter leads to increase in fluid temperature and nanoparticle concentrations. The microrotation parameter *G* effects are explained in Figures 4(a) and 4(b). Velocity and angular velocity distribution profiles are increased when microroatation parameter *G* increases. Figures 5(a) and 5(b) depict temperature profile θ and concentration profile φ, for different values of Prandtl number *Pr*. One can find that temperature of nanofluid particles decreases with the increase in *Pr* for both the cases *S=2* and *S=0.5*, which implies viscous boundary layer is thicker than the thermal boundary layer and the reverse phenomenon is observed from Figure 5(b).

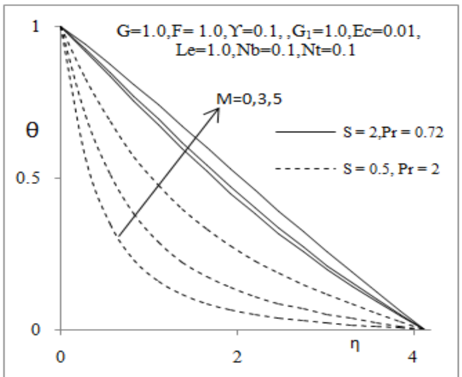

1(c). Temparature distribution for various values of M

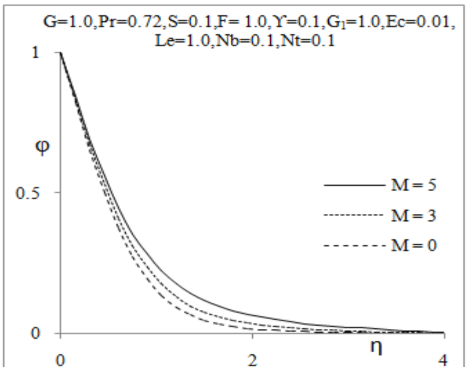

1(d). Concentration distribution for various values of M

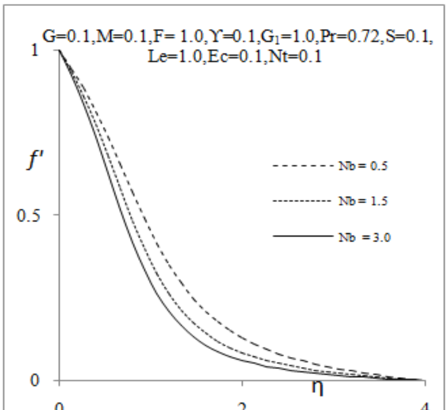

2(a). Velocity distribution for various values of Nb

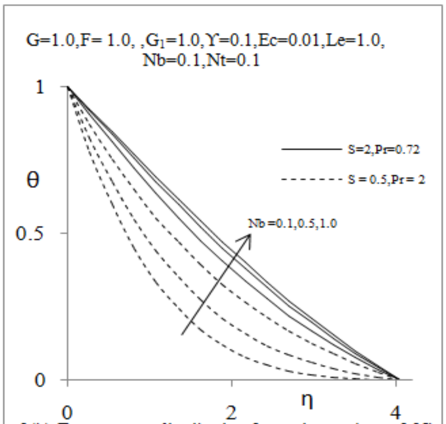

2(b).Temparature distribution for various values of Nb

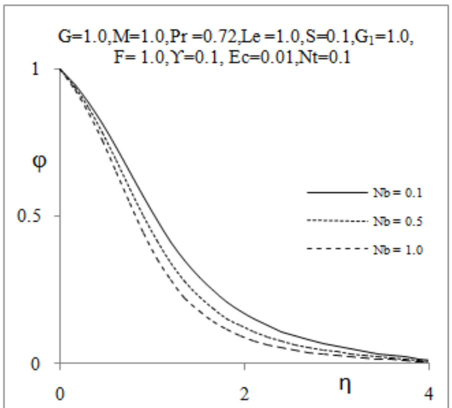

2(c).Concentration distribution for various values of Nb

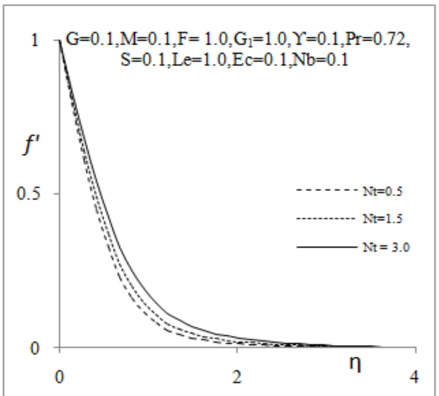

3(a) .Velocity distribution for various values of Nt

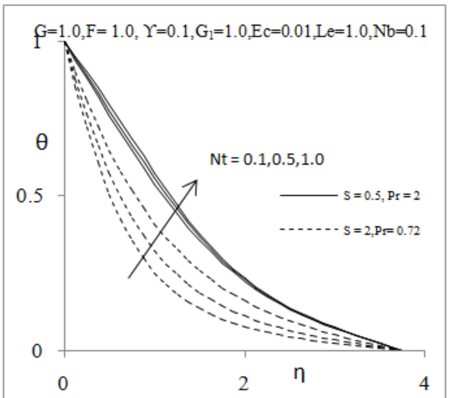

3(b). Temparature distribution for various values of Nt

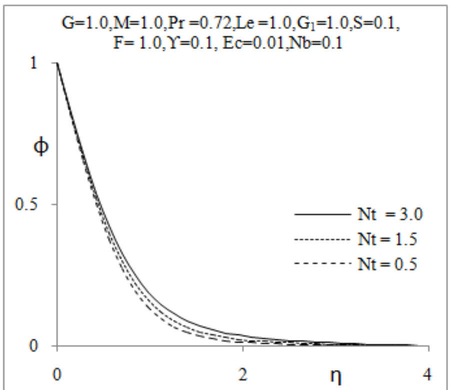

3(c). Concentration distribution for various values of Nt

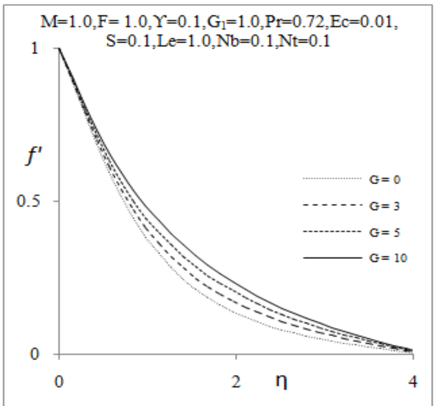

4(a). Velocity distribution for various values of G

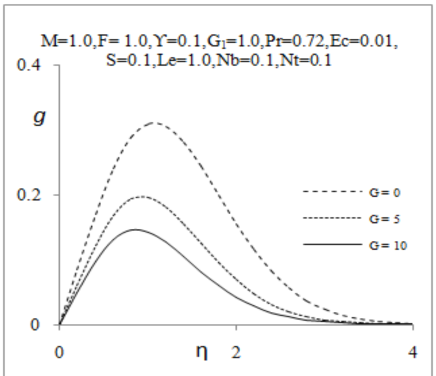

4(b). Angular velocity distribution for various values of G

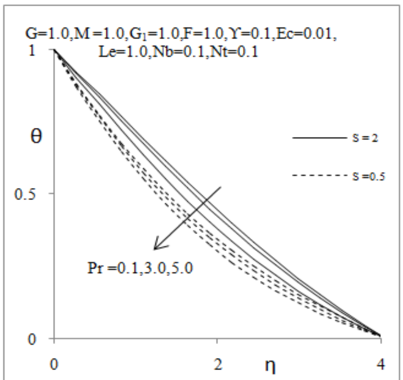

5(a).Temparature distribution for various values of Pr

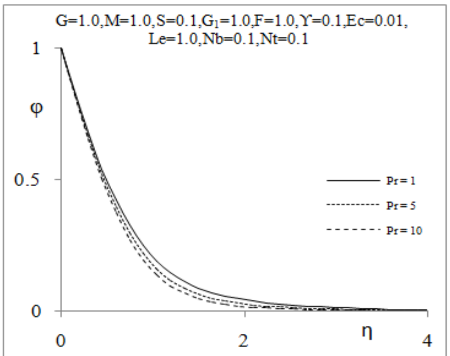

5(b). Concentration distribution for various values of Pr

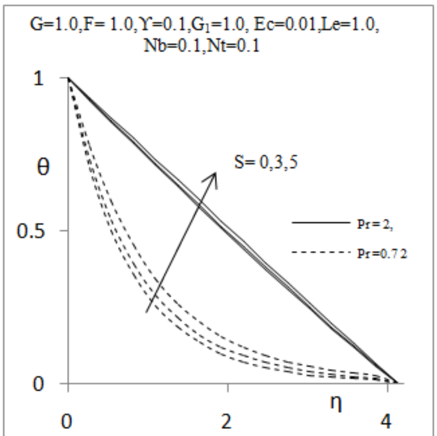

6). Temparature distribution for various values of S

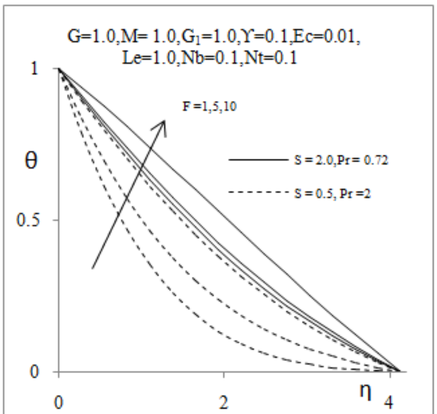

7). Temparature distribution for various values of F

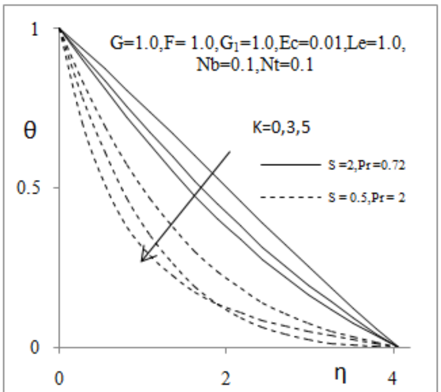

8).Concentration distribution for various values of ϒ

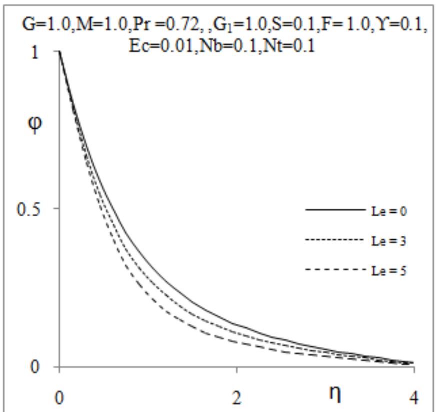

9). Concentration distribution for various values of Le

That is the concentration profiles are decreased as Prandtl number *Pr* increases. Fig. 6 shows the effect of the thermal conductivity parameter *S* on the temperature. From this figure it is noticed that the temperature decreases with the increasing of *S*. The variation of the temperature θ with respect to η for different values of *F* is plotted and shown in Fig.7. From Fig.7 one sees that the temperature decreases with θ increasing the radiation parameter *F*. The reason of this trend can be explained as follows. The effect of radiation is to decrease the rate of energy transport to the fluid, thereby decreasing the temperature of the fluid. Fig.8 illustrates the effect of the surface temperature parameter γ on the temperature distribution θ. From Fig.8, It is observed that the Concentration decreases as Chemical reaction parameter K increases. Lewies number *Le* effects are seen in Figure9, that is the Lewies number *Le*, decreases the concentration profiles when it increases.

REFERENCES

Ahmad, S. and Pop, I. 2010. Int. Commun. Heat Mass Transfer 37 987

Buongiorno, J. 2006. *ASME J. Heat Transfer* 128 240

Eastman, J. A., Choi, S.U. S., Li, S., Yu, W. and Thompson, L. J. 2001. *Appl. Phys. Lett*. 78 718

Eringen, A.C. 1972. Theory of thermomicro fluids, Math. Anal. 38 480–496.

Kuznetsov, A.V. and Nield, D.A. 2010. *Int. J. Theor. Sci.,* 49 243

Nield, D.A. and Kuznetsov, A.V. 2009. *Int. J. Heat Mass Transfer,* 52 5796

Raptis, A. 1998. Flow of a micropolar fluid past a continuously moving plate by the presence of radiation, *Int. J. Heat Mass* Transfer 41 2865–2866.

Schlichting, H. 1968. Boundary Layer Theory, McGraw-Hill, New York, 1968.

Slattery, J.C. 1972. Momentum, Energy and Mass Transfer in Continua, McGraw-Hill, New York, 1972.

Soundalgekar, V.M., Takhar, H.S. 1983. Flow of micropolar fluid past a continuously moving plate, *Int. J. Eng. Sci.,* 21 961–965.

Sparrow, E.M. Cess, R.D.1978. Radiation Heat Transfer, Hemisphere Publishing Corporation, Washington, DC, 1978.

Srinivas Maripala and Kishan Naikoti, 2016. MHD effects on micropolar nanofluid flow over a radiative stretching surface with thermal conductivity, *Advances in Applied Science Research,* 7(3):73-82.

Tzou, D.Y. 2008. ASME J. Heat Transfer 130 72401

****